IMPULSIVE, STOCHASTIC, AND SHOCK WAVE ACCELERATION OF RELATIVISTIC PROTONS IN LARGE SOLAR EVENTS OF 1989 SEPTEMBER 29, 2000 JULY 14, 2003 OCTOBER 28, AND 2005 JANUARY 20

J. PÉREZ-PERAZA[1], E. V. VASHENYUK[2], L. I. MIROSHNICHENKO[3], YU. V. BALABIN[2], AND A. GALLEGOS-CRUZ[4]
[1] Instituto de Geofísica, UNAM, C.U., Coyoacán, 04510, México, D.F., Mexico
[2] Polar Geophysical Institute, Apatity, Murmansk Region, 184209, Russia
[3] N.V. Pushkov Institute IZMIRAN, Moscow Region, 142190, Russia
[4] UPIICSA, I.P.N., Depto. de Ciencias Básicas, Té 950, Iztacalco, 08400, México D.F., Mexico
Received 2008 September 19; accepted 2009 January 14; published 2009 April 3

ABSTRACT

Using the data from neutron monitors and applying various techniques, the parameters of relativistic solar protons (RSPs) outside the magnetosphere are currently being derived by several research groups. Such data, together with direct proton measurements from balloons and spacecraft, allow the determination of particle energy spectra near the Earth's orbit in successive moments of time. Spectra of RSPs in a number of large solar events tend to indicate the existence of multistep acceleration at/near the Sun. In this paper, we study the generation of RSP by neutral current sheet, stochastic, and shock-wave acceleration, within the framework of two-component concepts for ground level enhancements (GLEs) of solar cosmic rays (SCRs). Our analysis is extended to large solar events (GLEs) of 1989 September 29, 2000 July 14, 2003 October 28, and 2005 January 20. We found two different particle populations (components) in the relativistic energy range: a prompt component (PC), characterized by an early impulselike intensity increase, hard spectrum and high anisotropy, and a delayed component, presenting a gradual late increase, soft spectrum and low anisotropy. Based on a two-source model for SCR spectrum formation at the Sun, we carried out theoretical calculations of spectra in the sources for both components. We conclude that the processes in neutral current sheet, together with stochastic acceleration in expanding magnetic trap in the solar corona, are able to explain the production of two different relativistic components. Shock acceleration in the presence of coronal mass ejection (CME) fits fairly only the nonrelativistic range of the SCR spectrum, but fails in the description of relativistic proton spectra, especially for the PC.

Key words: acceleration of particles – Sun: flares – Sun: particle emission

Online-only material: color figures

1. INTRODUCTION

Ground level events (GLEs) are characterized by the arrival on the Earth of relativistic solar particles (RSPs). Since 1942 to the present moment 70 GLEs have been observed. Using the ground-based worldwide neutron monitor (NM) network as a united multidirectional solar proton spectrometer in the relativistic energy domain, with data from no fewer than 25 NM stations and up to 40 (depending on particular events), the parameters of RSP in interplanetary space, as well as their dynamics in the course of a given GLE can be obtained. This is done by means of different modeling techniques and suitable computational codes for particle trajectories in the magnetosphere (e.g., Shea & Smart 1982; Bieber et al. 2005; Vashenyuk et al. 2003; 2007a; 2007b): the parameters of RSP in interplanetary space, as well as their dynamics in the course of a given GLE have been obtained with the help of different those techniques. In almost all cases, a comparison of the results from different authors shows the close similarity of spectra, anisotropy axes, pitch angle distributions (PADs), and other parameters. In most of these events (at least those of solar cycles 21–23), the spectra at the early stage of the events are hard, just at the time when the PAD in these events are the most narrow; as the PAD widen with time, the spectra become softer, creating a very peculiar exponential energy dependence. However, as time elapses, the spectra again get gradually steeper, up to the moment when they reach the steady state (Figures 1 and 2). Typical values of PAD in the course of time are, for instance, 0.17–11.82 in the 2003 October 28 event, and 0.4–25.0 for

the 2005 January 20 event (Vashenyuk et al. 2005c, 2005b). Based on their observation of the two-peak structure of solar proton intensity profiles, as can be seen in figures published in a series of papers as for instance Vashenyuk et al. (1994, 2002) Figure 1 shows explicitly the case of fluxes recorded at Goose Bay station. The previous authors have advanced the hypothesis that the data can be interpreted in terms of two distinct particle populations (components) in the relativistic energy range: a prompt component (PC), characterized by an early impulselike intensity increase, rigid spectrum and high anisotropy, followed by a delayed component (DC), presenting a gradual late increase, soft spectrum, and low anisotropy. The existence of two RSP populations is also confirmed by different forms of spectral fitting for PC and DC and by their dynamics, as derived from NM data with optimization methods: the PC energy spectrum follows an exponential form, while the DC energy spectrum may be fitted by a power-law function.

Such spectral shapes lead us to infer that the PC originates from acceleration in impulsive direct electric field acceleration and the DC, from stochastic acceleration. Since the PC and DC have different spectra and anisotropy characteristics, they are presumably connected to different sources at/near the Sun. Theoretical energy spectrum of particles, on basis to stochastic acceleration, has been derived in the past, only in partial energy ranges: analytical expressions for the nonrelativistic and ultra-relativistic domains, and numerical work in the transrelativistic domain. Some time ago we succeeded in deriving analytical expressions for the time-dependent energy spectrum of stochastically accelerated particles in the whole energy range of solar
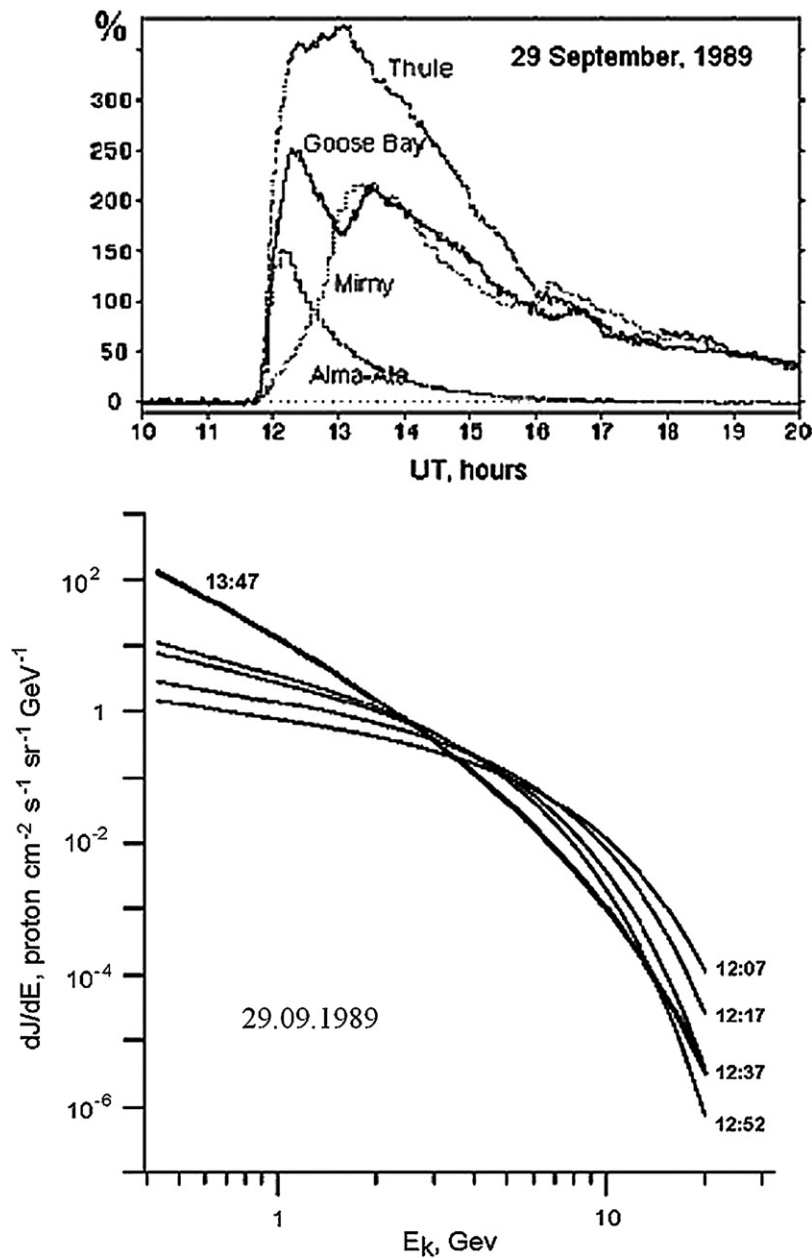
Figure 1 Top panel shows the time profile of protons according to NM data (Vashenyuk et al. 2000). The bottom panel shows observational energy spectra: the thin lines relate to the first ejection from the Sun. The thicker line is the spectrum of the second peak (Vashenyuk & Miroshnichenko 1997)).

particles That was achieved by solving the momentum-diffusion equation by means of the WKBJ method, Gallegos-Cruz & Pérez-Peraza (1995). On the other hand, we also derived the energy spectra of solar flare particles accelerated by impulsive direct electric fields in magnetic neutral current sheet (MNCS) topologies in solar flares, Pérez-Peraza et al. (1977, 1978). Here we apply such a spectral formalism to fit observational data of four GLEs of the solar cycles 22 and 23, and from there we derive the plausible source and acceleration parameters.

2. OXBSERVATIONS: DATA ON GLEs

In a series of papers (e.g., Vashenyuk et al. 2000), the technique for obtaining the energy spectra of relativistic protons from NM data has been described. This method has allowed the derivation of observational spectra outside the magnetosphere. Table 1 shows the derived spectra at different relativistic energy

bands for the four events under consideration. The time refers to the phase of maximum intensity (DC) of GLEs. Units of proton intensity are in $(cm^{-2}\ s^{-1}\ sr^{-1}\ MeV^{-1})$. Furthermore, as mentioned before, the procedure has led to the establishment of two components during RSP development. A list of the spectra of both components, the PC and DC of GLEs of the solar cycles 21–23 and the huge GLE of 1956 February 23, is given in the two last columns of Table 2, where the date, onset time of type II radio burst, flare importance and helio-coordinates of the flare are also indicated. The onset time of the type II radio emission corresponds to the start of energy release presumably related to its Hα eruption and start of CME, Manoharan & Kundu (2003). The type II onset is also a marker of relativistic proton acceleration, Cliver et al. (1982). Analyzing the evolution of their spectral form, each of the displayed events has revealed the PC and DC of RSPs. The best description of the PC spectrum is provided by exponential forms $J_{PC} = J_0 \exp(-E/E_0)$, where
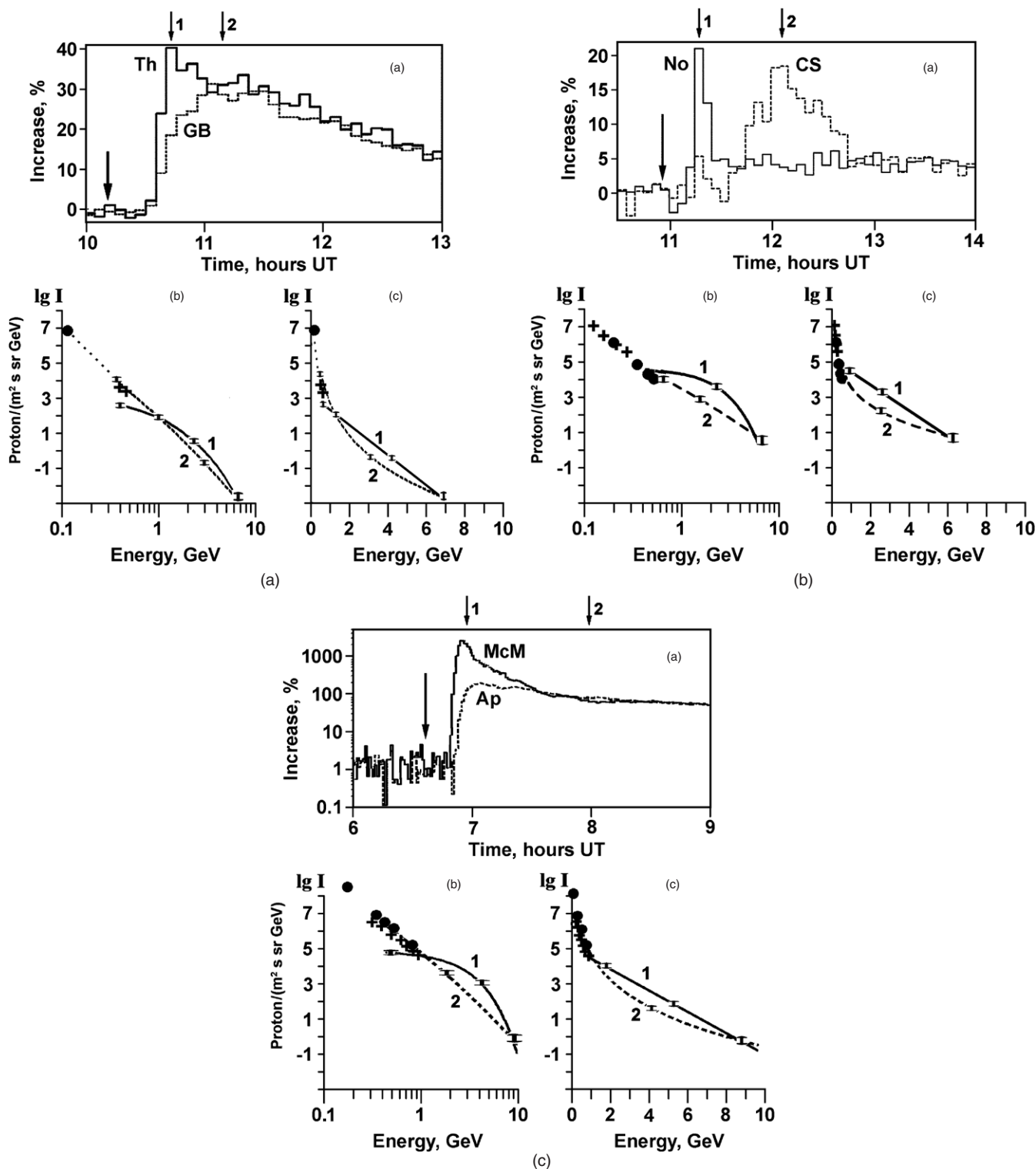
Figure 2 (a) Top panel (a) shows the time profile of protons of the "Bastille Day" GLE according to NM data of Thule and Goose Bay stations (Vashenyuk et al. 2006). The bottom panels show the energy spectra at two times, 10:38 and 11:00 UT are related to the (PC) and (DC), respectively (Vashenyuk et al. 2007b): panels (b) and (c) are in double logarithmic and semilogarithmic scales, respectively. (b) The top panel shows the time profile of protons of the 2003 October 28, according to NM data of Norilsk and Cape Schmidt stations (Vashenyuk et al. 2006). The bottom panel shows the energy spectra. The solid curve (1) corresponds to the PC, and the dashed line (2) to the DC: panels (b) and (c) are in double logarithmic and semilogarithmic scales, respectively. Direct solar proton data is represented by crosses (balloons) and blackened dots (*GOES-10* spacecraft). (c) The top panel shows the time profile of protons of the 2005 January 20 GLE according to NM data of McMurdo and Apatity stations (Vashenyuk et al. 2006). The bottom panel shows the energy spectra at two different times: spectra 1 at 7:00 UT and 2 at 8:00 UT correspond to the PC and DC, respectively (Vashenyuk et al. 2007b): panels (b) and (c) are in double logarithmic and semilogarithmic scales, respectively. Direct solar proton data at 8:00 UT are represented by crosses (balloons), and black dots (*GOES-11* spacecraft).

E_0 is characteristic proton energy. As to the DC, its spectrum may be fitted by power-law forms $J_{DC} = J_1 E^{-\gamma}$ (Table 2).

The corresponding parameters of the PC and DC spectra are displayed in the last four columns of Table 2, where

Table 1
Observational Energy Spectra of RSP at Different Energy Bands from NM Data with their Corresponding Error Bands in the Range (500–10^4 MeV)

E (GeV)	1989 Sep 9 13:35 UT		2000 Jul 14 11:00 UT		2003 October 28 11:55 UT		2005 January 20 7:25 UT	
0.5	3.67×10^{-3}	$\pm 1.8 \times 10^{-3}$	9.70×10^{-2}	$\pm 4.9 \times 10^{-3}$	3.96×10^{-3}	$\pm 1.7 \times 10^{-3}$	5.51×10^{-1}	$\pm 2.7 \times 10^{-1}$
0.6	1.71×10^{-3}	$\pm 8.5 \times 10^{-4}$	3.49×10^{-2}	$\pm 1.7 \times 10^{-2}$	2.09×10^{-4}	$\pm 1.0 \times 10^{-4}$	1.78×10^{-1}	$\pm 9.0 \times 10^{-2}$
0.7	8.95×10^{-4}	$\pm 1.8 \times 10^{-4}$	1.47×10^{-2}	$\pm 7.3 \times 10^{-3}$	1.22×10^{-4}	$\pm 6.0 \times 10^{-4}$	6.85×10^{-2}	$\pm 3.4 \times 10^{-2}$
0.8	5.11×10^{-4}	$\pm 2.5 \times 10^{-4}$	6.98×10^{-3}	$\pm 3.5 \times 10^{-3}$	7.64×10^{-4}	$\pm 3.8 \times 10^{-4}$	2.99×10^{-2}	$\pm 1.5 \times 10^{-3}$
0.9	3.11×10^{-4}	$\pm 1.5 \times 10^{-4}$	3.61×10^{-3}	$\pm 1.8 \times 10^{-3}$	5.06×10^{-4}	$\pm 2.5 \times 10^{-4}$	1.44×10^{-2}	$\pm 7.0 \times 10^{-3}$
1.0	2.00×10^{-4}	$\pm 1.0 \times 10^{-4}$	2.00×10^{-3}	$\pm 1.0 \times 10^{-5}$	3.50×10^{-4}	$\pm 1.7 \times 10^{-4}$	7.50×10^{-3}	$\pm 3.7 \times 10^{-5}$
2.0	1.09×10^{-5}	$\pm 5.0 \times 10^{-5}$	4.12×10^{-5}	$\pm 2.0 \times 10^{-6}$	3.09×10^{-5}	$\pm 1.5 \times 10^{-5}$	1.02×10^{-4}	$\pm 5.0 \times 10^{-6}$
3.0	2.00×10^{-6}	$\pm 1.0 \times 10^{-6}$	4.26×10^{-6}	$\pm 2.1 \times 10^{-7}$	7.48×10^{-6}	$\pm 3.7 \times 10^{-6}$	8.26×10^{-6}	$\pm 4.1 \times 10^{-7}$
4.0	5.92×10^{-7}	$\pm 3.0 \times 10^{-7}$	8.50×10^{-7}	$\pm 4.2 \times 10^{-7}$	2.73×10^{-6}	$\pm 1.3 \times 10^{-7}$	1.39×10^{-6}	$\pm 7.0 \times 10^{-7}$
5.0	2.23×10^{-7}	$\pm 1.1 \times 10^{-7}$	2.44×10^{-7}	$\pm 1.2 \times 10^{-6}$	1.25×10^{-6}	$\pm 6.0 \times 10^{-7}$	3.48×10^{-7}	$\pm 1.7 \times 10^{-8}$
6.0	1.08×10^{-7}	$\pm 5.0 \times 10^{-6}$	8.78×10^{-5}	$\pm 4.4 \times 10^{-6}$	6.62×10^{-7}	$\pm 3.3 \times 10^{-7}$	1.12×10^{-7}	$\pm 5.0 \times 10^{-8}$
7.0	5.64×10^{-8}	$\pm 2.5 \times 10^{-8}$	3.70×10^{-5}	$\pm 1.8 \times 10^{-3}$	3.86×10^{-7}	$\pm 1.9 \times 10^{-7}$	4.32×10^{-6}	$\pm 2.1 \times 10^{-9}$
8.0	3.22×10^{-8}	$\pm 1.5 \times 10^{-8}$	1.75×10^{-6}	$\pm 9.0 \times 10^{-3}$	2.42×10^{-7}	$\pm 1.2 \times 10^{-7}$	1.86×10^{-6}	$\pm 9.0 \times 10^{-9}$
9.0	1.96×10^{-8}	$\pm 1.0 \times 10^{-8}$	9.06×10^{-5}	$\pm 4.5 \times 10^{-3}$	1.60×10^{-7}	$\pm 8.0 \times 10^{-3}$	9.09×10^{-5}	$\pm 4.5 \times 10^{-9}$
10	1.26×10^{-8}	$\pm 5.0 \times 10^{-9}$	5.02×10^{-5}	$\pm 2.5 \times 10^{-3}$	1.11×10^{-7}	$\pm 5.0 \times 10^{-3}$	4.73×10^{-5}	$\pm 2.4 \times 10^{-9}$

Note. Proton intensity is in units of MeV^{-1} cm^{-2} s^{-1} sr^{-1}.

Table 2
Observational Energy Spectra of RSP of Several Events of Solar Cycles 21–23, Together with the Huge Event of 1956 February 23

No	Date	Type II Onset	Flare Importance	Helioco-Ordinates	PC Spectrum (Exponencial)		DC Spectrum (Power Law)	
					J_0 (cm^{-2} s^{-1} sr^{-1} MeV^{-1})	E_0 (MeV)	J_1 (cm^{-2} s^{-1} sr^{-1} MeV^{-1})	γ
1	1956 February 23	03:31	3B	N23W80	1.4×10^{-1}	1300	4.2×10^{-1}	5.2
2	1978 May 7	03:27	1B/X2	N23W82	1.4×10^{-3}	1650	. . .	. . .
3	1982 December 7	23:44	1B/X2.8	S19W86	1.5×10^{-2}	350	$2.o \times 10^{-4}$	3.2
4	1984 February 16	08:58	. . .	- W132	. . .	. . .	1.6×10^{-3}	6.2
5	1989 September 29	11:33	-/X9.8	- W105	1.6×10^{-3}	1850	2.0×10^{-4}	4.2
6	1989 October 19	12:58	4B/X13	S27E10	7.0×10^{-4}	650	4.0×10^{-3}	4.5
7	1989 October 22	18:05	2B/X2.9	S27W31	1.0×10^{-2}	620	5.0×10^{-4}	4.2
8	1990 May 21	22:19	2B/X5.5	N35W36	6.3×10^{-4}	830	2.7×10^{-4}	4.1
9	1997 November 6	11:55	2B/X9.4	S18W63	7.3×10^{-4}	1200	5.0×10^{-4}	4.3
10	2000 July 14	10:20	3B/X5.7	N22W07	1.1×10^{-3}	680	2.0×10^{-3}	5.6
11	2001 April 15	13:19	2B/X14.4	S20W85	2.0×10^{-2}	480	2.0×10^{-4}	5.1
12	2003 October 28	11:02	4B/X17.2	S16E08	1.4×10^{-3}	590	1.5×10^{-3}	4.4
13	2003 November 2	17:03	2B/X8.3	S14W56	1.5×10^{-4}	780	8.0×10^{-4}	6.0
14	2005 20 January	06:44	2B/X7.1	N14W61	1.5×10^{-2}	720	7.5×10^{-3}	6.2
15	2006 December 13	02:26	2B/X3.4	S06W24	1.6×10^{-3}	330	4.4×10^{-3}	5.5

Notes. Onset of type II radio emission is related to its Hα eruption and the start of CME (usually assumed that correspond to the start of suprathermal energy release). Proton intensity is in units of MeV^{-1} cm^{-2} s^{-1} sr^{-1}.

characteristic energies E_0 are given in units of MeV and proton intensities J_0 and J_1, in units of MeV^{-1} cm^{-2} s^{-1} sr^{-1}. Figure 1 illustrates the energy spectra at different moments in time for the events of 1989 September 29. Figure 2 shows the spectra for the Bastille Day (2000 July 14), 2003 October 28, and 2005 January 20 events, combining NM data with balloon and satellite data.

The two-peak structure measurements for the 1989 September 9 event was discussed in Miroshnishenko (2001), Vashenyuk & Miroshnichenko (1997, 2000). The spectra resulting from the techniques referred in the previous section, for the prompt and delayed fluxes are respectively: $J_{PC} = 1.6 \times 10^{-3} \exp(-E/1850)$ and $J_{DC} = 2 \times 10^{-4} E^{-4.2}$, in units of MeV^{-1} cm^{-2} s^{-1} sr^{-1}. Torsti et al. (1991, 1992) have also discussed the spike structure for this particular event. The Bastille Day event measurements were discussed in Vashenyuk et al. (2001), Pchelkin et al. (2001), and Vashenyuk et al. (2007b); the resulting spectra are $J_{PC} = 1.1 \times 10^{-3} \exp(-E/680)$ and $J_{DC} = 2 \times 10^{-3} E^{-5.6}$ in units of MeV^{-1} cm^{-2} s^{-1} sr^{-1}. The data for the 2003 October 28 event were discussed in Vashenyuk et al. (2005c) and Pérez-Peraza et al. (2006); the resulting spectra are $J_{PC} = 1.4 \times 10^{-3} \exp(-E/590)$ and $J_{DC} = 1.5 \times 10^{-3} E^{-4.4}$ in units of MeV^{-1} cm^{-2} s^{-1} sr^{-1}. The data for the 01.20.2005 event were discussed in Vashenyuk et al. (2005a, 2005b); the resulting spectra are $J_{PC} = 1.5 \times 10^{-2} \exp(-E/720)$ and $J_{DC} = 7.5 \times 10^{-3} E^{-6.2}$ in units of MeV^{-1} cm^{-2} s^{-1} sr^{-1}. It should be mentioned that multiple peak structure in SEP was also discussed in Shea & Smart (1996, 1997) and Cramp et al. (1997). Furthermore, Nemzek et al. (1994) show that such a kind of structure is preserved down to energies as low as 15 MeV.

3. THE SOURCE ACCELERATION SPECTRA

3.1 Direct Electric Field Acceleration in a Magnetic Neutral Current Sheet (MNCS)

The energy spectrum of solar protons from impulsive acceleration by a direct electric field in an MNCS was derived long ago by Pérez-Peraza et al. (1977, 1978) for several topologies in solar flares. The steady-state solution is

$$N(E) = N_o(E/E_c)^{-1/4} \exp[-1.12(E/E_c)^{3/4}] \quad (1)$$

with $N_o = 8.25 \times 10^5 \, (nL^2/B)(1/E_c)$ protons/MeV assuming anomalous conductivity; $E_c = 1.792 \times 10^3 \, (B^2L/n)$ MeV, B, L, and n are the magnetic field strength, the length of the sheet and number density, respectively.

3.2 Stochastic Acceleration

The transport equation describing the evolution of energetic particles in the energy phase-space is generally worked out by the well-known generalized Fokker–Planck-type equation. Analytical time-dependent and stationary solutions of that equation were derived by Gallegos-Cruz & Pérez-Peraza (1995) based on the WKBJ method. These analytical solutions embrace all energy ranges, unifying previous efforts in partial ranges developed by other researchers: the nonrelativistic, transrelativistic (numerically by Monte Carlo methods), and ultrarelativistic. Assuming an injection spectrum $Q(E, t) = q(E)\Theta(t) \approx q(E)$ (where $\Theta(t)$ is the step function), and escaping rate τ^{-1}, the general solution given by those authors is

$$N(E, t) = \frac{D^{1/4}(E)}{(4\pi)^{1/2}} \int_{E_o}^{E} \frac{e^{-R_1(E_o, E')}}{D^{3/4}(E')} \times \left[\frac{N(E', t)}{t^{1/2}} \right.$$
$$\left. \times e^{-at - R_2(E_o, E')/t} + \left(\frac{\pi}{4a}\right)^{1/2} q(E')R_3(E_o, E') \right] dE. \quad (2)$$

In this derivation, the authors have assumed the systematic acceleration process of the Fermi type $\langle dE/dt \rangle = \alpha\beta\varepsilon$, with the acceleration efficiency α (s^{-1}), and diffusion rates of $\langle dE^2/dt \rangle = \alpha\beta^2\varepsilon$, where $\beta = v/c$ is the particle velocity in terms of the light speed, and $\varepsilon = E + mc^2$ is the total energy of particles, m is a particle rest mass. The first term on the right side of Equation (2) (in the parentheses) represents the contribution to $N(E, t)$ of an instantaneous injection at time $t = 0$, whereas the second term describes the contribution arising from a continuous energy injection. The factors $R_1(E_0, E')$, $R_2(E_0, E')$, and $R_3 (E_0, E')$ are integral functions, which depend explicitly on the systematic energy gain (and energy loss) rate $<dE/dt>$ and on the diffusion rate $\langle dE^2/dt \rangle$, which both characterize the process of stochastic acceleration, Pérez-Peraza & Gallegos-Cruz (1994). Such a solution is exhaustively discussed in terms of Equations (15), (26), (41) in Gallegos-Cruz & Pérez-Peraza (1995). For the present calculations we will use hereafter Equation (2) for the particular case of MHD turbulence, with monoenergetic injection, and $D(p) \sim p^2/\beta$, corresponding to Equation (41) of the previous reference. Recently, Equation (2) has been solved analytically by Pérez-Peraza et al. (2006) with the same WKBJ method, using an additional term that describes the adiabatic cooling in the systematic energy change rate. There was assumed an adiabatic deceleration rate $\langle dE/dt \rangle = -\rho\beta^2\varepsilon$, where $\rho = (2/3)(V_r/R)$ s^{-1} is the adiabatic cooling efficiency, V_r is the velocity expansion, and $R(t)$ is the linear extension of the expanding magnetic structure. Assuming a mono-energetic continuous injection $q(E) = q_o\delta(E - E_{inj})$, $E \rightarrow E_{inj} = E_o$, Equation (2) becomes

$$N(E, t) = \frac{kq_o}{2} \left(\frac{3}{4\pi a}\right)^{1/2} \frac{\varepsilon^{3/4}[\varepsilon^2 - m^2c^4]^{-\frac{3\rho}{2\alpha}}}{(\varepsilon^2 - m^2c^4)^{1/8}}$$
$$\times \{[\text{erf}(z_1) - 1] \, e^{(3a/\alpha)^{1/2}J} + [\text{erf}(z_2) + 1]e^{-(3a/\alpha)^{1/2}J}\}, \quad (3)$$

where $k = \dfrac{\left[\varepsilon_o + \sqrt{\varepsilon_o^2 - m^2c^4}\right]^{3\rho/2\alpha}}{\varepsilon_o^{1/4} \left(\varepsilon_o^2 - m^2c^4\right)^{5/8}}$, $Z_{1,2} = (at)^{1/2} \pm R_2t^{-1/2}$,

$R_2 = (1/2)J(E)$

$$J(E) = (3/\alpha)^{1/2}\left\{ \tan^{-1} \beta^{1/2} - \tan^{-1} \beta_o^{1/2} \right.$$
$$\left. + 0.5 \ln \left[\frac{(1 + \beta^{1/2})(1 - \beta_o^{1/2})}{(1 - \beta^{1/2})(1 + \beta_o^{1/2})} \right] \right\},$$

$$a(E, \tau) = \tau^{-1} + 0.5 \, [F(\beta_o) + F(\beta)] \, , \, F(\beta)$$
$$= \frac{\alpha}{3}(\beta^{-1} + 3\beta - 2\beta^3) - \rho(2 - \beta^2),$$

β_0 is the value of β at the injection energy E_0, ε is the total energy and erf is the error function. In principle, both terms in Equations (2) and (3) contribute to the total spectrum at solar level; however, in practice, the contribution from initial injection ($N_o \neq 0$) is negligible. For $\rho = 0$, Equation (3) reduces to Equation (41) in Gallegos-Cruz & Pérez-Peraza (1995). Spectra in Equations (2) and (3) tend to a power-law form in the high-energy range as the time elapses toward the steady state situation ($t \rightarrow \infty$).

4. RESULTS AND DISCUSSION

The direct confrontation of theoretical source spectra with observational spectra, ignoring transport effects on the particle fluxes, is conventionally based on the following approximations.

1. We deal with relativistic protons which in practice do not see interplanetary magnetic structures.
2. Fluxes are considered at the t_m, the time of maximum intensity.
3. Many events occur in well-connected Sun–Earth flares.
4. For events which are far from the Sun–Earth connection helio-longitude connection, a model-dependent assumption is considered: a closed expanding coronal magnetic structure connects particle fluxes with the 60° W Sun–Earth connection (e.g., Figure 7.25 in Miroshnichenko 2001).

For fittings to the DC spectra with Equations (2) and (3) we assume here: (1) a supra-Alfvénic monoenergetic injection energy at energy E_o, (Equation (2)), (2) similar to (1) with the addition of adiabatic losses (Equation (3)), and (3) a more realistic injection by pre-acceleration in an MNCS, with a well-defined spectrum of the type of Equation (1), according to the solution of the transport equation given in Gallegos-Cruz & Pérez- Peraza (1995) (Equations (50) and (51)). For fittings to the PC we use here Equation (1). The results are shown in Figures 3–7.

Figures 7(a) and (b) show the time-dependent spectra for the 2003 October 28 event at an acceleration time of 10 s, when the steady state has not yet been reached, and at 20 s, when it has already been reached. Fixing the injection energy $E_0 = 1$ MeV and the mean confinement time $\tau = 1$ s, the fitting is carried out by testing the best values of the free parameters (α and ρ) that best reproduce the spectral data. Assumption (1) corresponds to the case of pure acceleration, with no energy losses ($\rho = 0$), whereas the second (2) corresponds to a finite value of ρ. The parameters $\alpha(t)$ and $\rho(t)$ are in fact functions of time, however, the value of ρ has been constrained by assuming a velocity expansions V_r in the range of 400–4000 km s^{-1}, e.g., Gopalswamy et al. (2005) and linear extensions of the expanding acceleration volume of $(10^{-2} - 1)$ solar radius.
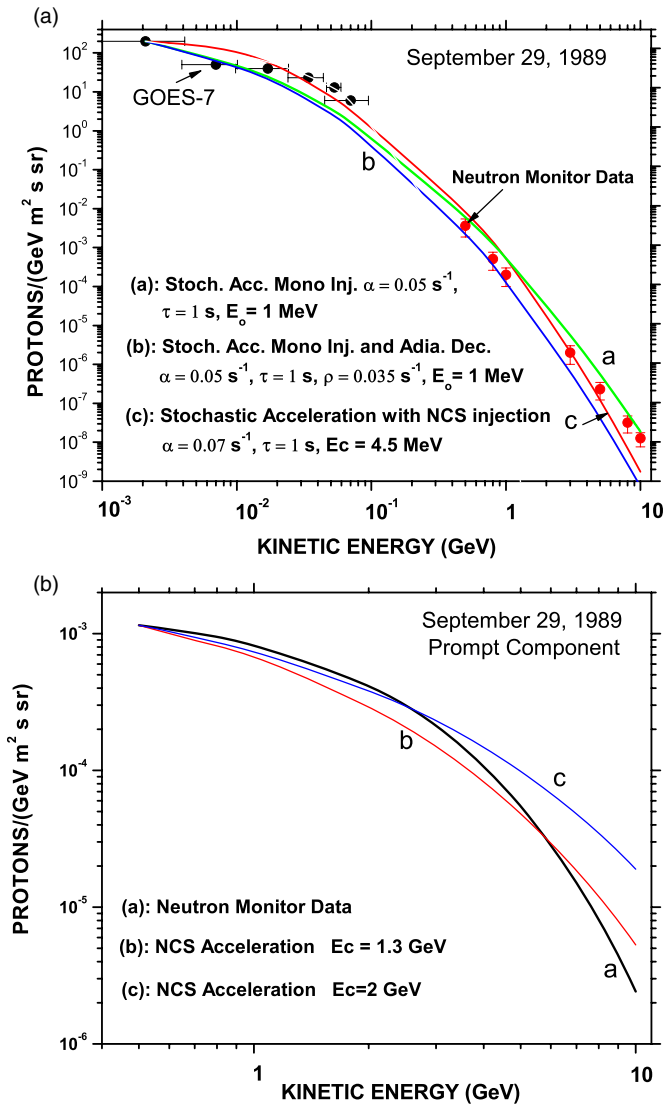
Figure 3 (a) Fitting of the experimental energy spectrum (circles with error bars) of the DC of the 1989 September 29 event, by the theoretical source spectra: ignoring (a) and including (b) adiabatic losses (Equations (2) and (3) respectively at the steady state limit). Curve (c) corresponds to Equation (2) with MNCS injection of the type of Equation (1). The employed data come from the list of NM stations given in Vashenyuk & Miroshnichenko (1997) and Miroshnichenko (2001). (b) Fitting of the experimental energy spectrum of the PC of the 1989 September 29 GLE by the theoretical source spectra, Equation (1).

(A color version of this figure is available in the online journal.)

Figure 4 (a) Fitting of the experimental energy spectrum (circles with error bars) of the DC of the 2000 July 14 GLE, by the theoretical source spectra: ignoring (b) and including (c) adiabatic losses (Equations (2) and (3) respectively at the steady state limit). Curve (a) corresponds to Equation (2) with MNCS injection of the type of Equation (1). The list of NM stations employed is given in Vashenyuk et al. (2001), Pchelkin et al. (2001), and Vashenyuk et al. (2007b). (b) Fitting of the experimental energy spectrum of the PC of the 2000 July 14 GLE by the theoretical source spectra, Equation (1).

(A color version of this figure is available in the online journal.)

For fittings of Equation (1) to the PC spectra, we have limited the free parameter E_c to the following range of values: $B = 50$–100 Gauss, $L = (10^{-3}$–$10^{-2})$ solar radius, and $n = (10^9$–$10^{10})$ cm^{-3}.

An analysis of Figures 3–7 shows that adiabatic acceleration was not important for these events, indicating that the acceleration was relatively high and the expansion velocity, relatively low. It can also be seen that the best fit is systematically obtained when the injection is achieved with a well defined pre-acceleration spectrum from an MNCS and not with monoenergetic injection. Moreover, the fitting of the PC with acceleration from thermal energies in an MNCS shows that, within the error bars, the spectra are well reproduced. Let us exemplify our results with one of the studied events, that of 2003 October 28, illustrated in Figures 5 and 7: according to the proposed
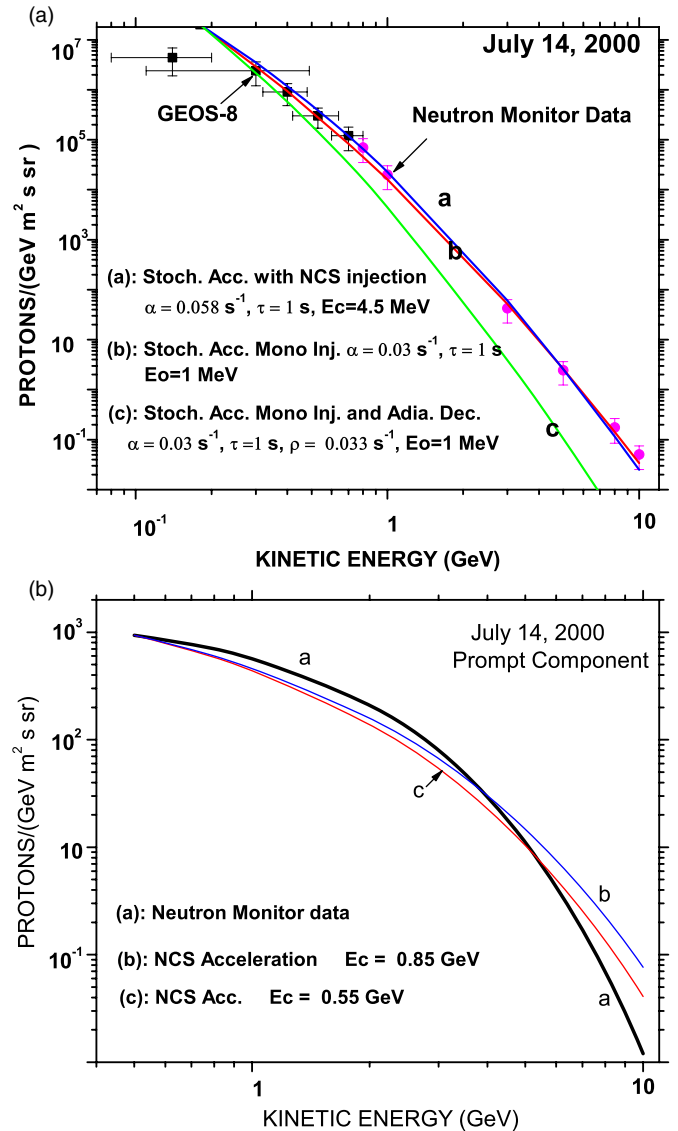
scenario the DC is generated into a closed expanding magnetic structure, that during such an expansion gets in touch with other loops, one of which may be of opposite polarity, creating an MNCS, where local particles in its diffusion region are impulsively accelerated by the deterministic electric fields produced in the process of magnetic reconnection (Miroshnichenko et al. 1996). Such deterministically accelerated particles are seen at the Earth around 11:20 UT as a PC (Figures 2(b) and 5(b)). The enclosed component in the expanding structure (undergoing stochastic acceleration by the generated turbulence in the expanding plasma) is susceptible of losing energy by adiabatic cooling while they are being accelerated: assuming the magnetic loop associated with the flare begins to expand around 11:02 (according to the type II radio onset of the B/X17.2/S16 E08 flare), and taking into account that relativistic particles last
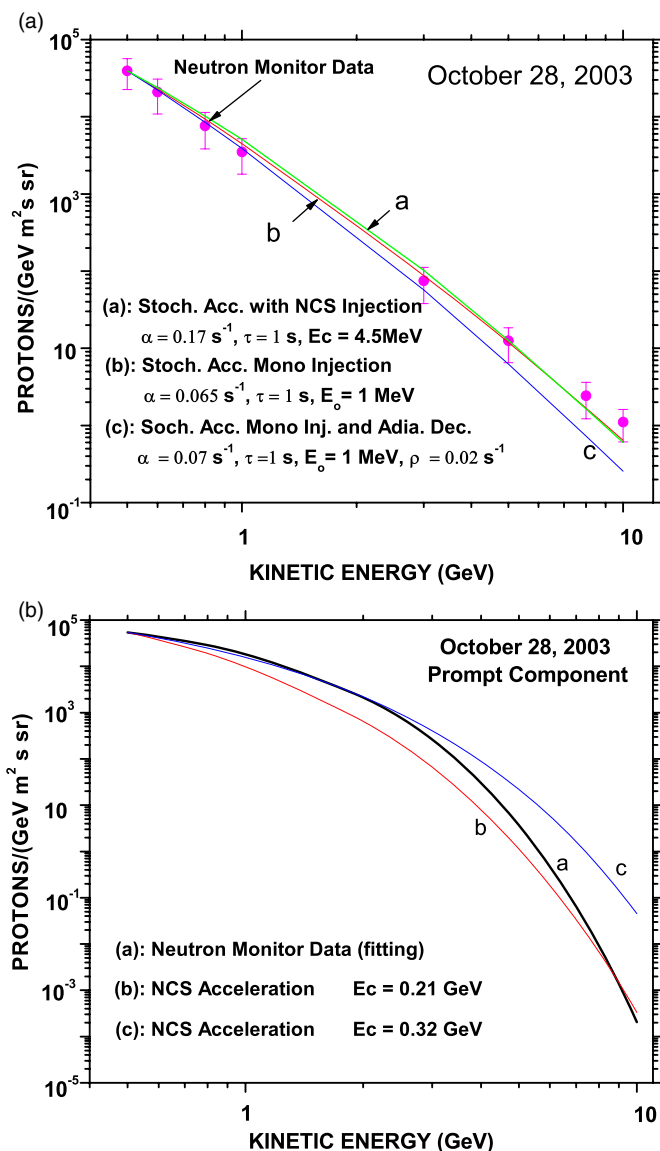
Figure 5 (a) Fitting of the experimental energy spectrum (circles with error bars) of the DC of the 2003 October 28 GLE, by the theoretical source spectra: ignoring (b) and including (c) adiabatic losses (Equations (2) and (3) respectively at the steady state limit). Curve (a) corresponds to Equation (2) with MNCS injection of the type of Equation (1). The list of NM stations employed is given in Vashenyuk et al. (2005c) and Pérez-Peraza et al. (2006). (b) Fitting of the experimental energy spectrum of the PC of the 2003 October 28 GLE by the theoretical source spectra, Equation (1).
(A color version of this figure is available in the online journal.)

Figure 6 (a) Fitting of the experimental energy spectrum (circles with error bars) of the DC of the 2005 January 20 GLE, by the theoretical source spectra: ignoring (b) and including (c) adiabatic losses (Equations (2) and (3) respectively at the steady state limit). Curve (a) corresponds to Equation (2) with MNCS injection of the type of Equation (1). The list of NM stations employed is given in Vashenyuk et al. (2005a, 2005b). (b) Fitting of the experimental energy spectrum of the PC of the 2005 January 20 GLE by the theoretical source spectra, Equation (1).
(A color version of this figure is available in the online journal.)

about 8 minutes to reach the Earth, the first bunch was measured at 11:40 UT (Pérez-Peraza et al. 2006). They must have been generated before ∼11:32 when the acceleration efficiency $\alpha(t)$ has reached a value enough high to overcome the energy loss barrier, say $\alpha_1 \approx 0.09$ s^{-1} and the observed particles have spent about 4 s under this acceleration efficiency. Later after 10 s, the stochastic process efficiency decreases to a value $\alpha_2 \approx 0.07$ s^{-1} such that particles measured at 12:00 UT (Figure 7(a)) have been accelerated under this efficiency regime. Finally, after 20 s of acceleration, the efficiency decreases to $\alpha_3 \approx 0.065$ s^{-1} where the steady state ($\alpha \approx$ constant) is practically being reached; the magnetic structure is open, turbulence is dissipated and particles, under this stationary regime are measured at about 12:10 UT, (Figure 7 (b)). Since under the present scenario, the expansion begins around 11:00 UT and the stroke to the collat-
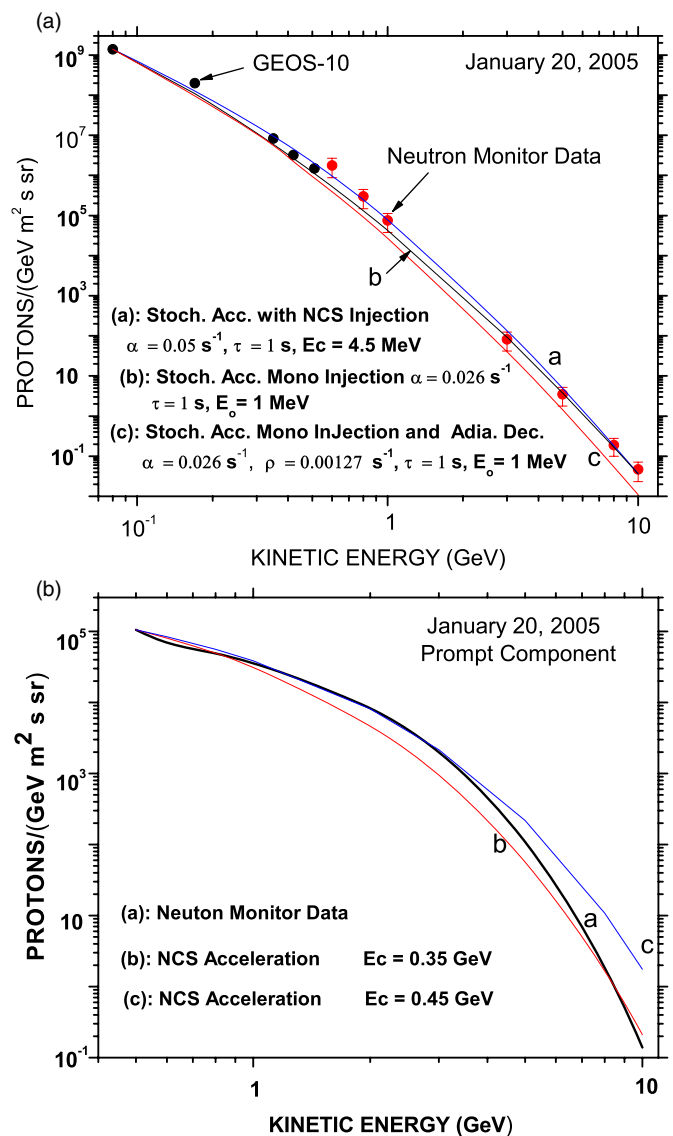
eral loop occurs at ∼11:10 UT (particles of this PC are measured at the Earth at 11:20), this implies that the population in the expanding bottle has been about half an hour undergoing adiabatic cooling, competing with the stochastic acceleration process, up to the moment that efficiency reach the value α_1 and begin to escape with a mean escape time of about 1 s.

Concerning *shock acceleration* two outstanding works dealing only with the DC should be mentioned here: in Berezhko & Taneev (2003), the derived energy spectrum is unable to fit the relativistic high-energy data from NM data from the 1989 September 29 event, or, alternatively, if it is fitted, then it does not fit the transrelativistic energy range (see their Figure 6). It is shown in Bombardieri et al. (2006, 2008), for the 2000 July 14 and 20.01.2005 events that using the formulation given in Gallegos-Cruz & Pérez-Peraza (1995), the observational spec-
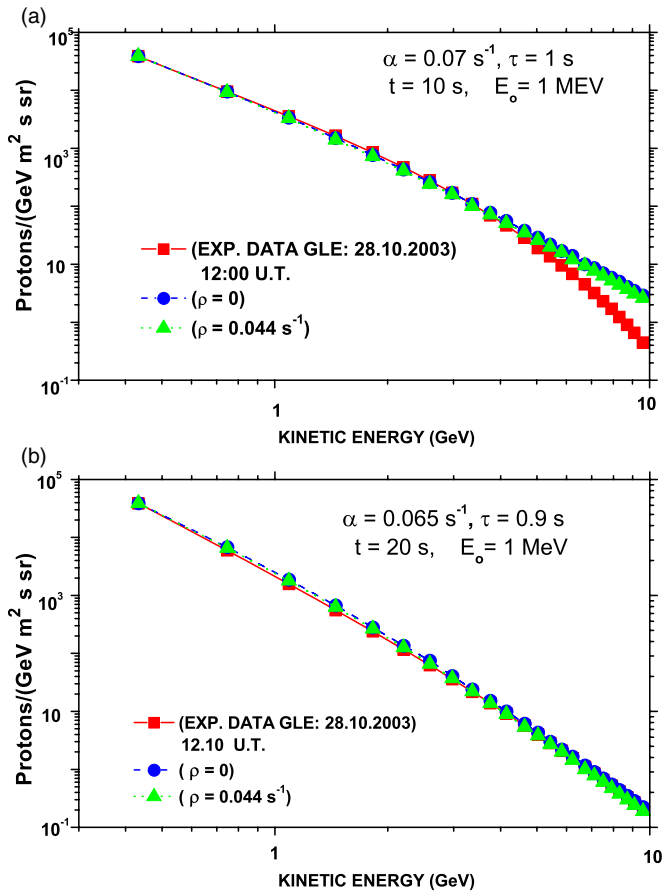
Figure 7 (a) Fitting the experimental energy spectrum (squares) of the DC of the 2003 October 28 GLE using the time-dependent spectra (Equations (2) and (3)), with monoenergetic injection, while considering and ignoring adiabatic losses (triangles and circles respectively): at $t = 10$ s the steady state is not yet reached. (b) Idem (a) at $t = 20$ s when the steady state is already reached.

(A color version of this figure is available in the online journal.)

trum is best reproduced by stochastic acceleration, rather than with shock acceleration (see Figure 8 in Bombardieri et al. 2006 and Figures 7, 8, and 10 in Bombardieri et al. 2008).

Regarding the scenario of particle production in RSP events, since the PC and DC have different spectra and anisotropy characteristics, they are probably connected to various sources at/near the Sun, Pérez-Peraza et al. (1992). Considering the timing of the generation and release of the two components from the solar corona, the proposed scenario for the RSP events is based on two different sources of particle acceleration: the fact that particle ejection is highly abrupt (coronal storage time ≈ 0) and particle flux is highly anisotropic (sharp rise in intensity and rapid decay) points toward a source associated with open field lines (rapid particle escape), where the particles are efficiently accelerated by a deterministic process, and rapidly collimated toward the IMF lines as a focusing particle bunch. Such acceleration may occur during magnetic merging of coronal field lines of opposite polarity creating an MNCS. Local particles in the sheet diffusion region are impulsively accelerated by the deterministic electric fields produced during the process of magnetic reconnection. This phase takes place during the initial energy release and is linked with the Hα eruption and the onset of CME, along with type II radio emission. Particles of DC are originally trapped in magnetic arches in the low corona and then are accelerated by a stochastic mechanism from the MHD turbulence into the expanding flare plasma. Accelerated

particles of DC can be then carried out to the outer corona by an expanding CME. They are released into interplanetary space after a period of from 30 minutes to 2 hr, at which time the magnetic trap is destroyed giving rise to the source of accelerated particles that is extended in time and azimuth.

5. CONCLUSIONS

We have shown that the energy spectra of the PC in RSP events with two distinct populations can be adequately reproduced by an exponential type spectrum from MNCS acceleration. In the case of the DC component, the spectra may be adequately reproduced by stochastic acceleration, and under conditions of very low acceleration efficiency, adiabatic losses could eventually contribute to shaping the spectrum, which is not the case with the four events under consideration. It must be emphasized that we could not predict in advance that adiabatic cooling would not have any noticeable effect, because we ignored, a priori, the values of our free parameter α. It was just at the moment of doing the best fits that we found that the required α values were the same in both cases (with $\rho = 0$ and $\rho \neq 0$) even though the spectra were quite distinguishable. Though the values of α and ρ were in the same order, the worst fitting of data was systematically obtained with adiabatic deceleration as can be seen in Figures 3(a)–6(a). That leads us to infer that any plasma-expanding phenomenon, such as a CME-driven shock wave, was not related to the stochastic acceleration stage.

We have also shown that a realistic injection spectrum of pre-accelerated particles in an MNCS in the flare body into the stochastic acceleration process reproduces the observational spectrum better than the conventional assumption of a monoenergetic injection at ~1 MeV. It should be emphasized that in reproducing the PC and DC spectra, the derived source parameters and the parameter of acceleration efficiency from our fittings are within the realistic values expected in the coronal flare. Therefore, we have derived the plausible source and acceleration parameters of the four studied events.

Finally, it is worth mentioning that the presence of CME indicates the possible production of RSP in a shock acceleration process, as has been suggested by other authors (in particular for the 1989 September 29 event; e.g., Lovel et al. 1998). Though this is undoubtedly a process that is present, according to the results of Bombardieri et al. (2006, 2008) and Berezhko & Taneev (2003), we believe that it makes only a partial contribution to the low-energy part of the spectrum, which probably mixes with the bulk of particles of those making up the DC population. This assumption is based on the fact that shock acceleration fits only the low-energy region. On the other hand, to our knowledge, up to now shock acceleration has not been able to explain the PC.

REFERENCES

Berezhko, E. G., & Taneev, S. N. 2003, Astron. Lett., 29, 530
Bieber, J. W., et al. 2005, in Proc. 29th Int. Cosmic Ray Conf., 1, 237
Bombardieri, D. J., et al. 2006, ApJ, 644, 565
Bombardieri, D. J., et al. 2008, ApJ, 682, 1315

Cliver, E. W., Kahler, S. W., Shea, M. A., & Smart, D. F. 1982, ApJ, 260, 362
Cramp, J. L., Duldig, M. L., Fluckiger, E. O., Humble, J. E., Shea, M. A., & Smart, D. F. 1997, JGR, 102, 24237
Gallegos-Cruz, A., & Pérez-Peraza, J. 1995, ApJ, 446, 400
Gopalswamy, N., Hie, H., Yashiro, S., & Usoskin, I. 2005, in Proc. 29th Int. Cosmic Ray Conf., 3, 101
Lovel, J. L., Duldig, M. L., & Humble, J. E. 1998, JGR, 103, 2373
Manoharan, P. K., & Kundu, M. R. 2003, ApJ, 592, 597
Miroshnichenko, L. I. 2001, Solar Cosmic Rays (Dordrecht: Kluwer)
Miroshnichenko, L. I., Pérez-Peraza, J., Rodríguez-Frías, D., Del Peral, L., Vashenyuk, E. V., & Gallegos-Cruz, A. 1996, AIP Conf. Proc., High Energy Solar Physics (New York: AIP), 374, 140
Nemzek, R. J., Belian, R. D., Cayton, T. E., & Reeves, G. D. 1994, JGR, 99, 4221
Pchelkin, V. V., Vashenyuk, E. V., & Gvozdevky, B. B. 2001, Proc. 27th Int. Cosmic Ray Conf., 8, 3379
Pérez-Peraza, J., Gálvez, M., & Lara, R. 1977, Proc. 15th Int. Cosmic Ray Conf., 5, 23
Pérez-Peraza, J., Gálvez, M., & Lara, R. 1978, Space Res., 18, 365
Pérez-Peraza, J., & Gallegos-Cruz, A. 1994, ApJS, 90, 669
Pérez-Peraza, J., Gallegos-Cruz, A., Vashenyuk, E. V., & Miroshnichenko, L. I. 1992, Geomagn. Aeron., 32, 1
Pérez-Peraza, J., Gallegos-Cruz, A., Vashenyuk, E., Balabin, E., & Miroshnichenko, L. I. 2006, Adv. Space Res., 38, 418
Shea, M. A., & Smart, D. F. 1982, Space Sci. Rev., 32, 251
Shea, M. A., & Smart, D. F. 1996, in AIP Conf. Proc. 374, High Energy Solar Physics, ed. R. Ramaty, N. Mandzhavidze, & X.-M. Hua (New York: AIP), 131
Shea, M. A., & Smart, D. F. 1997, Proc. 25th Int. Cosmic Ray Conf., 1, 129
Torsti, J., Eronen, T., Mahonen, M., Riihonen, E., Schultz, C. G., Kudela, K., & Kananen, H. 1991, Proc. 22nd Int. Cosmic Ray Conf., 3, 141
Torsti, J. J., Eronen, T., Mahonen, M., Riihonen, E., Schultz, C. G., Kudela, K., & Kananen, H. 1992, in Proc. of the 3rd COSPAR Colloquium, Solar Wind Seven, ed. E. Marsch & R. Schwenn (Oxford: Pergamon), 545
Vashenyuk, E. V., Balabin, Y. V., Bazilevskaya, G. A., Makhmutov, V. S., Stozhkov, Y. I., & Svirzhevsky, N. S. 2005a, Proc. 29th Int. Cosmic Ray Conf., 1, 213
Vashenyuk, E. V., Balabin, Y. V., & Gvozdevsky, B.B. 2003, Proc. 28th Int. Cosmic Ray Conf., 6, 3401
Vashenyuk, E. V., Balabin, Y. V., Gvozdevsky, B. B., Karpov, S. N., Yanke, V. G., Eroshenko, E. A., Belov, A. V., & Gushchina, R. T. 2005b, Proc. 29th Int. Cosmic Ray Conf., 1, 209
Vashenyuk, E. V., Balabin, Y. V., Gvozdevsky, B. B., Miroshnichenko, L. I., Klein, K. L., Trottet, G., & Lantos, P. 2005c, Proc. 29th Int. Cosmic Ray Conf., 1, 217
Vashenyuk, E. V., Balabin, Y. V., Miroshnichenko, L. I., & Pérez-Peraza, J. 2007a, Proc. 30th Int. Cosmic Ray Conf., 1, 249
Vashenyuk, E. V., Balabin, Y. V., Perez-Peraza, J., Gallegos-Cruz, A., & Miroshnichenko, L. I. 2006, Adv. Space Res., 38, 411
Vashenyuk, E. V., Balabin, Y. V., & Stoker, P. H. 2007b, Adv. Space Res., 40, 331
Vashenyuk, E. V., Gvozdevsky, B. B, Phelkin, V. V., Usoskin, I. G., Mursula, K., & Kovaltsov, G. A. 2001, Proc. 27th Int. Cosmic Ray Conf., 8, 3383
Vashenyuk, E. V., & Miroshnichenko, L. I. 1997, Proc. 25th Int. Cosmic Ray Conf., 1, 161
Vashenyuk, E. V., Miroshnichenko, L. I., & Gvozdevsky, B. B. 2000, Nuovo Cimento C, 23, 285
Vashenyuk, E. V., Miroshnichenko, L. I., Sorokin, M. O., Pérez-Peraza, J., & Gallegos-Cruz, A. 1994, Adv. Space Res., 14, 711
Vashenyuk, E. V., Pérez-Peraza, J., Miroshnichenko, L. I., & Pchelkin, V. V. 2002, Proc. The 6th World Multiconf. on System., Cybern. & Inform., 27, 443